



OPEN ACCESS

EDITED BY

Giovanna Romano,
Anton Dohrn Zoological Station, Italy

REVIEWED BY

Victor Hugo Hernandez Elizarraga,
Universidad Autónoma de Querétaro,
Mexico
Monica Saldarriaga,
Universidad Bernardo O'Higgins, Chile

*CORRESPONDENCE

Ana R. Díaz-Marrero
adiazmar@ipna.csic.es
José J. Fernández
jjfercas@ull.edu.es

†These authors have contributed
equally to this work

SPECIALTY SECTION

This article was submitted to
Marine Biology,
a section of the journal
Frontiers in Marine Science

RECEIVED 06 April 2022

ACCEPTED 16 September 2022

PUBLISHED 11 October 2022

CITATION

Nocchi N, González-Orive A,
Hernández-Creus A, Lorenzo-
Morales J, Rodríguez A, Morchón R,
Díaz-Marrero AR and Fernández J.J
(2022) Alciporin, a pore-forming
protein as complementary defense
mechanism in *Millepora alcicornis*.
Front. Mar. Sci. 9:914084.
doi: 10.3389/fmars.2022.914084

COPYRIGHT

© 2022 Nocchi, González-Orive,
Hernández-Creus, Lorenzo-Morales,
Rodríguez, Morchón, Díaz-Marrero and
Fernández. This is an open-access
article distributed under the terms of
the [Creative Commons Attribution
License \(CC BY\)](https://creativecommons.org/licenses/by/4.0/). The use, distribution
or reproduction in other forums is
permitted, provided the original
author(s) and the copyright owner(s)
are credited and that the original
publication in this journal is cited, in
accordance with accepted academic
practice. No use, distribution or
reproduction is permitted which does
not comply with these terms.

Alciporin, a pore-forming protein as complementary defense mechanism in *Millepora alcicornis*

Nathalia Nocchi^{1,2†}, Alejandro González-Orive^{3†},
Alberto Hernández-Creus³, Jacob Lorenzo-Morales^{4,5,6},
Adriana Rodríguez^{7,8}, Rodrigo Morchón⁹,
Ana R. Díaz-Marrero^{1,10*} and José J. Fernández^{1,2*}

¹Instituto Universitario de Bio-Orgánica Antonio González (IUBO AG), Universidad de La Laguna (ULL), La Laguna, Spain, ²Departamento de Química Orgánica, Universidad de La Laguna (ULL), La Laguna, Spain, ³Departamento de Química, Área de Química Física, Instituto de Materiales y Nanotecnología (IMN), Universidad de La Laguna (ULL), La Laguna, Spain, ⁴Instituto Universitario de Enfermedades Tropicales y Salud Pública de Canarias (IUETSPC), Departamento de Obstetricia y Ginecología, Pediatría, Medicina Preventiva y Salud Pública, Toxicología, Medicina Legal y Forense y Parasitología, Universidad de La Laguna (ULL), La Laguna, Spain, ⁵Red de Investigación Cooperativa en Enfermedades Tropicales (RICET), Madrid, Spain, ⁶Centro de Investigación Biomédica en Red de Enfermedades Infecciosas (CIBERINFEC), Instituto de Salud Carlos III, Madrid, Spain, ⁷Departamento de Biología Animal, Edafología y Geología, UD Ciencias Marinas, Facultad de Ciencias (Sección Biología), Universidad de La Laguna (ULL), La Laguna, Spain, ⁸Grupo de investigación BIOCON-IU ECOACUA, Facultad de Ciencias del Mar, Universidad de Las Palmas de Gran Canaria, Las Palmas, Spain, ⁹Zoonotic Diseases and One Health GIR, Laboratory of Parasitology, Faculty of Pharmacy, University of Salamanca (USAL), Salamanca, Spain, ¹⁰Instituto de Productos Naturales y Agrobiología (IPNA), Consejo Superior de Investigaciones Científicas (CSIC), La Laguna, Spain

Millepora alcicornis (Cnidaria: Hydrozoa), known as fire coral, is a tropical species settled in marine ecosystems of the Canary Islands in the last years. This hydrocoral biosynthesizes toxins involved in chemical defense and prey capture mechanisms. Toxicological studies have shown that the venom contained in the nematocysts of *Millepora* species is mainly composed of thermolabile proteins that display hemolytic activity, causing skin irritation and burn-like lesions upon contact. As a continuation of a previous study, the chromatographic fractionation of the aqueous extracts of *M. alcicornis* has confirmed the coexistence of proteins of different nature responsible for the hemolytic effects of red blood cells (RBCs) through two different mechanisms. Aside from the already described phospholipase A2 (PLA2) activity, in this work the presence of alciporin, a pore-forming protein (PFP), has been established for the first time for *M. alcicornis*. The sequence analysis revealed that alciporin fit an actinoporin with high homology to stichotoxins. The hemolytic effects of alciporin were analyzed and sphingomyelin was identified as its biological target. Also, the evolution of the hemolytic damage produced at the nanoscale has been studied using atomic force microscopy (AFM).

KEYWORDS

alciporin, pore-forming protein, pore-forming toxin, *Millepora*, AFM

1 Introduction

The intense maritime traffic and global change effects is causing range expansions of many species that can now tolerate living beyond their normal limit of distribution (Fleds et al., 1993; Harley et al., 2006). Tropical species arrive to temperate areas, such as Canary Islands, increasing their distribution and causing serious environmental concern for the conservation of the ocean, altering functions and services delivered by local ecosystems (Bax et al., 2003; Thomsen et al., 2015). This is the case of *Millepora alcicornis* (Linnaeus, 1758), which arrived at the Canary Islands 13 years ago (Clemente et al., 2011) from the Caribbean region (López et al., 2015; Rodríguez et al., 2019). *M. alcicornis* (Cnidaria: Hydrozoa: Milleporidae) is a hydrocoral known as fire coral, their colonies are colonial, polypoid hydrocorals secreting a calcareous skeleton that are an important structural component of tropical coral reefs (Lewis, 2006). Their distribution is amphi-Atlantic, from Brazil, Bermuda to Ascension Island, Cape Verde Islands, Canary Islands and Madeira Island (Laborel, 1974; Clemente et al., 2011; Hoeksema et al., 2017; Wirtz and Zilberberg, 2019). In general, it is frequent in tropical regions where it plays an important role in the organization of coastal benthic communities (Lewis, 2006). In 2008, three colonies were recorded in Tenerife Island, Canary Islands (Clemente et al., 2011). A monitoring has been done on this specie from 2008 to the present, observing an increase in the number de colonies, cover and localities where has been registered (Rodríguez, 2019a; Rodríguez et al., 2019).

In Canary Islands, *M. alcicornis* is present in two localities of Tenerife Island, El Poris (28° 10' 24.12'' N, 16° 25' 47.12'' W) from 2008 year (Clemente et al., 2011) and Caletillas (28° 22' 52'' N; 16° 21' 18'' W) from 2021 year (Figure 1 and Figures S1–S5). Experimental studies on *M. alcicornis* from Tenerife Island have showed its high tolerance to ocean acidification conditions and higher growth rates under high temperature (Rodríguez,

2019b). In future scenarios of climate change, where a rise of temperature is expected, *M. alcicornis* can become a winner species under climate change conditions.

The nematocysts of these marine hydrozoans can penetrate the human skin and produce lesions similar to burns. These injuries provoke irritation, burning or stinging pain, erythematous and edematous dermatitis, pruritus, hives, and skin necrosis. In addition, *Millepora* species can induce systemic symptoms consist of malaise, nausea, vomiting, abdominal pain, muscle spasm, diarrhea, respiratory difficulty, tachycardia, hypotension, and fever (Jouiaei et al., 2015). These effects are attributed to the secretion of enzymes, potent pore forming toxins and neurotoxins contained in cnidarians nematocysts. Toxicological studies have shown that the venom contained in the nematocysts of *Millepora* species is mainly composed of thermolabile proteins that display hemolytic activity (Olguín-López et al., 2019). Also, small peptide sequences below 10 kDa obtained from the hemolytic proteome of *M. complanata* have shown antimicrobial properties against Gram-positive and Gram-negative bacteria (Hernández-Elizárraga et al., 2022). Despite the hemolytic activities of several cnidarian venoms are well documented (Jouiaei et al., 2015), the importance or implications of the mechanisms of *in vivo* erythrocyte lysis triggered by venom hemolysins is still not completely understood. In fact, local tissue damage induced by cnidarians such as inflammation is attributed to hemolysins injected by the nematocysts. For this reason, it is important to study the hemolytic properties of the complex cnidarian venoms, which could lead to better care for the victims (Iguchi et al., 2008; Mariottini and Pane, 2013; Lourenço, 2020). However, up to now, the mechanism of the envenomation caused by these species has not been completely defined.

Recently, we described the hemolytic effects induced by the aqueous extract of *M. alcicornis* in rat erythrocytes (Díaz-Marrero et al., 2019). In this work, the hemolytic effects (hemolytic unit 50 (HU) 50 59 ng/mL) observed when rat



FIGURE 1
Detail and colonies of the fire coral *Millepora alcicornis* from Tenerife Island.

erythrocytes were incubated in the presence of the aqueous extract (68.0 µg protein/mg lyophilized extract) of this coral, were mainly attributed to phospholipase A2 (PLA2) activity. PLA2 was the main component in the aqueous extract of *M. alcicornis* with an estimated molecular mass around 20 kDa. PLA2 is a known enzyme also found in snakes and other venoms and body fluids that chemically cleaves glycerophospholipids at the sn-2 position to yield a lysophospholipid and a fatty acid as reaction products. With the use of atomic force microscopy (AFM), we were able to visualize in detail the complete hemolytic process at the nanoscale level describing the mode of action of PLA2 proteins on the structure of rat red blood cells (RBCs). Additionally, it should be noted that superficial damages of different nature were also observed on cell membranes. Those damages seemed to point out to the fact that an additional hemolytic mechanism could be contributing to the hemolytic effects of the aqueous extracts of the fire coral *M. alcicornis* on RBCs. Those effects seemed to be related to the presence of Pore-Forming Proteins (PFPs). As a continuation of our previous study, in this work we aimed to confirm the existence of a PFP that may contribute to the hemolytic activity of the aqueous extracts of *M. alcicornis*. Thus, we isolate, characterize, and analyze the hemolytic behavior of the PFP, named as alciaporin. The mechanism of the resultant arc-pore was studied at nano scale level using AFM techniques. The use of AFM is revealed as a powerful tool to understand the potential of cnidarians venoms in biological processes.

2 Materials and methods

2.1 Biological material

A combination of different fragments of branches, tips, and stems from *M. alcicornis* colonies (2-5 cm, 1 Kg) were collected by SCUBA diving at a 6–8 m deep at El Porís, Tenerife Island (28°10'24.12"N, 16°25'47.12"W) in September 2018. After collection, the colonies were kept wet with sea water and immediately transported to laboratory where was stored at –20 °C for later use in protein extraction.

2.2 Extraction and purification of the pore-forming proteins toxins

To obtain crude protein extract from *M. alcicornis* colonies, nematocyst discharge was induced in the laboratory as described by Diaz-Marrero et al. (2019). Initially, 1 Kg of frozen coral fragments were removed from the –20 °C freezer and kept together in deionized water under stirring at 4°C for 24 hours. Afterward, the fragments were removed, and the resultant suspension was filtered and centrifuged twice at 3000 rpm for 15 min at 4 °C using a Thermo Scientific Sorvall RC6 + centrifuge

(F14S-6 × 250X rotor). This procedure of keeping the fragments in deionized water, filtration and centrifugation was repeated three times. At the end supernatants were combined and lyophilized, yielding a single aqueous crude protein extract (13.8 g) from pooled fragments. The supernatant (crude protein extract) was freeze-dried and stored at –20 °C. Then, for of the pore-forming proteins toxins, 135 mg of lyophilized crude protein extract (62.5 µg protein/mg extract determined as described by Diaz-Marrero et al. (2019) was solubilized in 400 µL of 10 mM commercial phosphate (PBS) buffer (pH 7.2) (SIGMA DIAGNOSTICS®). The solution was centrifuged at 5000 rpm for 20 min at 4 °C. Next, this supernatant was filtered through a 0.2 µm PVDF syringe sterile filter (Whatman™, 13 mm) and chromatographed. The purification was performed on a gel filtration chromatography with a Toyopearl® HW-50F (TOSOH®; 30–60 µm; 500–20,000 Da MW range) resin column (190 x 10 mm, death volume ~ 15mL) equilibrated with 10 mM PBS buffer (pH 7.2) (SIGMA DIAGNOSTICS®). The column was eluted at a flow rate of 0.9 mL/min and 0.45 mL fractions were collected in tubes. The absorbance of each tube was monitored at 210, 254, 280, 365 and 545 nm (BioTeK, Power Wave XS). The sample in the tubes were pooled together according to their absorbance profile, and freeze-dried to yield three final fractions (F1, F2 (alciaporin) and F3). All steps were carried out at 4°C and fractions F1, F2 y F3 were stored at -20°C until required.

2.3 Isolation of red blood cells

The RBCs samples used in all *in vitro* hemolytic assays and in atomic force microscopy were collected from the coccygeal artery of Sprange Dawley rats anesthetized with isoflurane in tubes that containing EDTA as anticoagulant (BD Vacutainer K3E 15%, Aprotinin 250 KIU, Ref. 361017). The samples were kept at 4°C until their use.

2.4 Hemolytic activity assays

In vitro study of the hemolytic properties against Sprange Dawley rats' erythrocytes of the fractions obtained from the chromatographic process of the aqueous extract of *M. alcicornis* was performed on 96-well plates. Briefly, the fractions were tested in serial dilutions in PBS with RBCs washed three times with saline solution, with final concentrations ranging from 100 to 0.195 µg/mL. Saline solution and TritonX (0.1%) was used as negative and positive control of hemolysis in the experiment, respectively. The samples were incubated at 37°C for 45 minutes. Unlysed erythrocytes were pelleted by centrifugation, and the absorbance of the supernatant was measured at 405 nm to determine the hemoglobin released from lysed erythrocytes. One hemolytic unit (HU50) was defined as the amount of protein sample required to cause 50% hemolysis. Results were

normalized to 100% hemolysis with positive control. All experiments were performed in triplicate.

2.5 Atomic Force Microscopy analysis

Atomic Force Microscopy (AFM) was used for the detailed study at the nanoscale of the action of Pore-Forming Proteins on the membrane of RBCs. Briefly, 200 μL of fresh rat erythrocytes were incubated different times ($t=1, 5, 10,$ and 30 min) with 20 μL of the most active protein fractions, F1 y F2 (alciporin), at a final concentration of 100 $\mu\text{g}/\text{mL}$ and $7 \cdot 10^9$ erythrocytes/mL. After each incubation time, 10 μL of the treated blood sample was smeared on glass slides. Samples were dried for 10 min before AFM analysis.

AFM topographic images were obtained in Peak Force mode using a Dimension Icon microscope with a Nanoscope V control unit from Bruker. Scan rates of 0.5–1.2 Hz and ScanAsyst-Air-HR (140–160 kHz, and $0.4\text{--}0.6 \text{ N}\cdot\text{m}^{-1}$) tips (from Bruker) were used (Espinoza et al., 2018). To get representative information about the hemolysis process of the RBCs, images from ($100 \times 100 \mu\text{m}^2$) to ($0.6 \times 0.6 \mu\text{m}^2$) were recorded using 512 points/line. AFM image analysis software from Bruker and from Gwyddion were used for image processing. For the analysis of the RMS roughness, diameter, and depth of the pores induced in the cell membrane after F2 exposure, a minimum of 50 pinholes from at least three different RBCs for every exposure time were considered. Blue marks in the images and related dashed lines in the cross-section profiles are displayed in the AFM figures to illustrate the height ranges to be taken into account.

2.6 Sphingomyelin inhibition assays

A sample of fraction F2 (alciporin) (3.42 mg) was reconstituted in saline solution at a concentration of 1000 $\mu\text{g}/\text{mL}$ and divided into two equal parts, one of them containing an excess of sphingomyelin (2.80 mg; 1:1.6). Both samples were kept at 0°C for 60 min. An aliquot of 20 μL of each sample was added into 200 μL of rat blood to reach a final concentration of 100 $\mu\text{g}/\text{mL}$ of protein and $7 \cdot 10^9$ erythrocytes/mL. Then, the smear was prepared for AFM analysis of the hemolytic effects after incubation times of 1, 5, 10, 15 and 30 min. For the inhibition hemolytic assays, a sample of 1.70 mg of alciporin was treated similarly, and divided into two equal fractions, one of them containing sphingomyelin (1:1.6) with final concentrations ranging from 100 to 0.195 $\mu\text{g}/\text{mL}$. The assay was performed in triplicates as described in section 2.4.

2.7 Protein identification

2.7.1 Samples preparation

Samples of alciporin (F2) were dissolved in 100 μL of distilled water and quantified by Qubit (Life technologies,

Madrid, Spain). 7 μL of samples ($\sim 0.8 \mu\text{g}/\mu\text{L}$) were mixed with PBS buffer 0.5M to 20 μL of final volume. Cysteine residues were reduced by 2 mM DTT in 50 mM PBS buffer at 60°C for 20 min. Sulfhydryl groups were alkylated with 5 mM IAA in 50 mM PBS in the dark at r.t. for 30 min. IAA excess was neutralized with 10 mM DTT in 50 mM PBS, 30 min at room temperature (r.t.). Samples were subjected to trypsin digestion with 150 ng of sequencing grade modified trypsin (Promega) in 50 mM PBS in thermomixer at 37°C , 4 hours. The reaction was stopped with TFA at a final concentration of 0.1%. The digestion mixtures were dried in a vacuum centrifuge, resuspended in 15 μL of 2% ACN, 0.1% TFA.

2.7.2 Liquid chromatography and tandem mass spectrometry

LC-MS/MS system composed of an Ekspert nanoLC 425 (Eksigent) and a mass spectrometer nanoESI qTOF (6600plus TripleTOF, ABSCIEX) were used. 5 μL of peptide mixture sample was loaded onto a trap column ($3 \mu\text{C}18\text{-CL} 120 \text{ \AA}$, $350 \mu\text{m} \times 0.5\text{mm}$; Eksigent) and desalted with 0.1% TFA at 5 $\mu\text{L}/\text{min}$ during 3 min. The peptides were then loaded onto an analytical column ($3 \mu\text{C}18\text{-CL} 120 \text{ \AA}$, $0.075 \times 150 \text{ mm}$; Eksigent) equilibrated in 5% ACN (acetonitrile) 0.1% FA (formic acid). Elution was carried out with a linear gradient of 10 a 40% B in A for 20 min. (A: 0.1% FA; B: ACN, 0.1% FA) at a flow rate of 300 nL/min. Sample was ionized in a Source Type: Optiflow < 1 μL Nano applying 3.0 kV to the spray emitter at 175°C . Analysis was carried out in a data-dependent mode. Survey MS1 scans were acquired from 350–1400 m/z for 250 ms. The quadrupole resolution was set to 'LOW' for MS2 experiments, which were acquired 100–1500 m/z for 25 ms in 'high sensitivity' mode. Following switch criteria were used: charge: 2+ to 4+; minimum intensity; 100 counts per second (cps). Up to 100 ions were selected for fragmentation after each survey scan. Dynamic exclusion was set to 15 s. Report included as Supplementary Material.

2.7.3 ProteinPilotv5.0. search engine (ABSciex)

ProteinPilot default parameters were used to generate peak list directly from 6600 plus TripleTOF wiff files. The Paragon algorithm (Shilov et al., 2007) of ProteinPilot v 5.0 was used to search the SwisProt (210106) and Uniprot-millepora (with 26,032 entries) databases with the following parameters: trypsin specificity, cys-alkylation, taxonomy non restricted, the search effort set to rapid, and FDR analysis. The protein grouping was done by Pro group algorithm (a protein group in a Pro Group Report is a set of proteins that share some physical evidence. Unlike sequence alignment analyses where full length theoretical sequences are compared, the formation of protein groups in Pro Group is guided entirely by observed peptides only. Since the observed peptides are determined from experimentally acquired spectra, the grouping can be considered to be guided by usage of spectra. Then, unobserved regions of protein sequence play no role in explaining the data. Proteins

showing unused score >1.3 were identified with confidence $\geq 95\%$. Report included as Supplementary Material. Homology higher than 97% were only considered when performing Blastp analysis. Sequences were edited and aligned using MEGA 5.0 software program (Tamura et al., 2011). Phylogenetic analyses were carried out using the methodology described by Reyes-Battle et al. (2014), with the MEGA 5.0 software program.

3 Results and discussion

M. alcornis is a tropical hydrocoral that has found the optimal environmental conditions to develop colonies in the marine ecosystems of the Canary Islands as consequence of climate change and the increase in maritime traffic due to globalization (Clemente et al., 2011). Fire corals are known to cause severe painful stings, burning sensation, and itching upon contact that may evolve with systemic effects such as gastrointestinal symptoms as well as respiratory difficulty, tachycardia, hypotension, and fever (Jouiaei et al., 2015). These symptoms cause discomfort to those involved in underwater, professional, and recreational activities related to tourism, thus causing a potential health risk. The study of toxins contained in the nematocysts produced by cnidarian cnidocytes is crucial to understand the mechanisms involved in this biological process.

In addition to the already described phospholipase A2 (PLA2) activity, precedents seem to point out to the fact that an additional hemolytic mechanism could contribute to the hemolytic effects observed on the aqueous extracts of *Millepora* species on RBCs (García-Arredondo et al., 2014). In the case of *M. complanata*, aside from the PLA2, the hemolytic activity has been suggested to be caused by trypsin, chymotrypsin, serine-proteases and matrix metalloproteases

(Hernández-Elizárraga et al., 2022). As part of an ongoing research on the hemolytic effects of hydrocoral *M. alcornis* using AFM, we observed that this mechanism could be attributed to the presence of pore-forming protein toxins (PFPs) (Díaz-Marrero et al., 2019). Therefore, to corroborate this hypothesis, the following specific objectives were proposed in this study: *i*) to conduct the purification of the PFPs in the aqueous extract of *M. alcornis*; *ii*) to establish the hemolytic effects of the resulting protein fractions using *in vitro* assays on rat erythrocytes; *iii*) to analyze the specific hemolytic effects of the active protein fractions on the membrane of RBCs using AFM; and *iv*) characterize the protein responsible for pore formation and determine its membrane target in rat RBCs.

Initially, to verify the aqueous crude protein extract hemolytic properties, hemolytic activity tests were carried out revealing a potent effect on rat erythrocytes with a hemolytic unit 50 (HU50) value of $5.01 \pm 0.66 \mu\text{g}$ of protein/mL. After fractionation of this extract, it was possible to get three main fractions according to the chromatogram obtained after absorbance measurements at 545 nm; F1: peak with retention time (RT) at 2.42 min, F2 (alcorpurin): peak at RT = 5.50 min and F3 (Figure S5). The hemolytic effects of these three fractions were also tested at different concentrations as described in the methodology section. The results obtained are shown in Figure 2, revealing that both F1 and F2 showed a concentration-dependent hemolytic activity while fraction F3 did not hemolyzed RBCs at any of the concentrations tested. F1 showed different hemolytic profile than F2 with an HU50 value of $1.75 \pm 0.42 \mu\text{g/mL}$. On the other hand, fraction F2 showed a different behavior reaching its maximum hemolytic effect (60%) at concentrations higher than 50 $\mu\text{g/mL}$.

In order to confirm the differentiated hemolytic effect of the protein fractions F1 and F2 atomic force microscopy (AFM) technique was employed. To confirm the mechanisms of

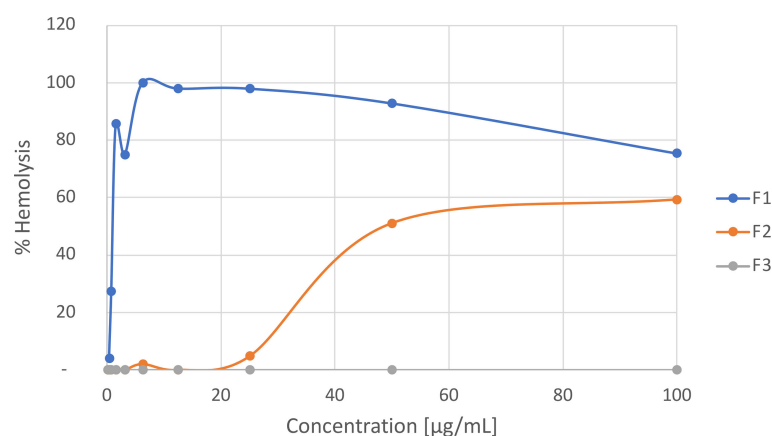


FIGURE 2
Hemolytic activity of protein fractions in *M. alcornis*.

hemolysis, rat erythrocytes were treated by adding an aliquot of both lyophilized fractions F1 and F2 in physiological saline solution and analyzed at different incubation times (1, 5, 10, 30 mins). Control measurements carried out on healthy RBCs are shown in the [Figure S6](#) in the Supporting Information (SI).

AFM analysis of the effect of F1 on the surface of RBC of rat showed that damages caused by this fraction correspond to those previously described for a phospholipase A2 mechanism ([Díaz-Marrero et al., 2019](#)). [Figure 3](#) shows a detail of the PLA2 hemolytic effects produced after 5 min, where superficial degradation of the outer and inner leaflets of the cell membrane are clearly observed. AFM images in [Figure 4](#), collected for $t = 1$ and 30 min, revealed the extension, development, and reproduction of the depth of the damages already reported in [Díaz-Marrero et al. \(2019\)](#). The presence of these damaged regions can be rationalized in terms of the hydrolysis reaction produced between the membrane phospholipids catalyzed by PLA2-type proteins from the coral extract. PLA2-type proteins specifically trigger the rupture of the ester bond at the sn-2 position of the glycerol backbone of phosphatidylcholine residues in the outer leaflet of the cell membrane.

The RMS roughness of the membrane surface inside the damaged membrane regions displayed in [Figure 4](#) showed an averaged value of 1.51 ± 0.43 nm, which is considerably higher than that registered for healthy cell membrane areas, i.e. 0.87 ± 0.20 nm, whose smoother morphology is shown in more detail in [Figure S7](#).

In the same way, AFM images of the effects observed after incubation of rat erythrocytes with the enriched fraction F2 of *M. alcicornis*, named as alciporin, were recorded, revealing a different mechanism than that for F1, as previously described ([Díaz-Marrero et al., 2019](#)). [Figure 5](#) shows detailed AFM images of the response of rat blood cells after 1 min treatment with F2. In this case, the damages observed on the membrane of an

isolated erythrocyte reveal punctual and deep damages distributed along the surface. A detailed analysis indicated the formation of adjacent concentric pores that seems to be the initial stages of a pore-formation mechanism. After 10 minutes of incubation, damages caused by alciporin are abundant and spread out on the surface of the cell membrane. In addition, bigger holes of higher dimensions than those observed after 1-minute incubation are present. [Figure 6](#) shows a detail of these small-sized pores, and the results (regarding width and depth) of the analysis of several cross-section profiles carried out on the latter are summarized in [Table 1](#). Interestingly, both the roughness and the overall dimensions of the circular pores noticeably increase with time, so does the pinhole surface coverage as can be seen in [Figure S8](#).

Together with the arising and the progressive development already mentioned for the small-sized pinholes, significantly bigger circular pores are also detected on the membrane of RBCs exposed to alciporin, as can be observed in [Figure 7A](#) and [Figure S9](#). Also, the analysis of these large-sized damages revealed the formation of neat circular pores reaching 205 nm wide and 65 nm deep. These data confirmed that alciporin causes damages of different nature on cell membranes through an additional hemolytic mechanism that could be attributed to PFPs. Interestingly, these wide pores in the membrane cells allow to distinguish in detail the spectrin network underneath. The latter is better depicted in [Figures 7B, C](#). It is noteworthy to mention that these large, dilated pores are not the consequence of the overlap/collapse of adjacent minor pinholes, which is illustrated in [Figures S10–S11](#), but the result of the development in a larger scale of the PFP model already discussed. The occurrence of the latter is detected even from $t = 1$ to 30 min.

Several studies have reported that porins proteins interact exclusively with sphingomyelin containing membranes ([Bakrač et al., 2008](#); [Črnigoj Kristan et al., 2009](#); [García-Ortega et al., 2011](#)). PFPs are present in Anthozoa and Hydrozoa. They

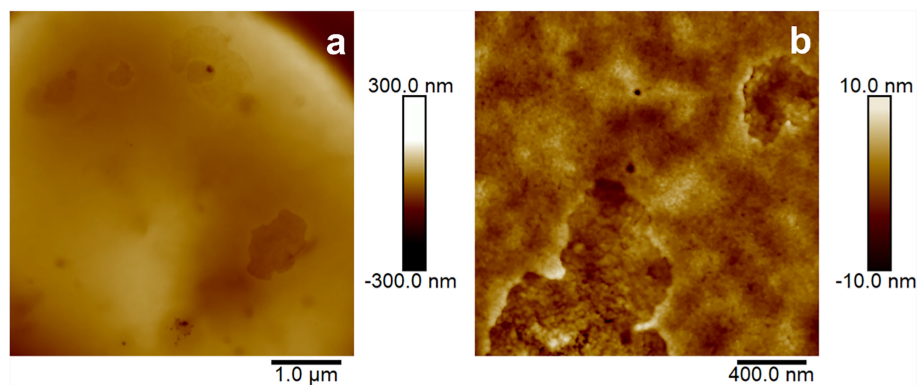


FIGURE 3
5.0 × 5.0 μm² (A) and 2.0 × 2.0 μm² (B) AFM images of the surface of RBC after being exposed to the hemolytic fraction F1 of *M. alcicornis* for $t = 5$ min.

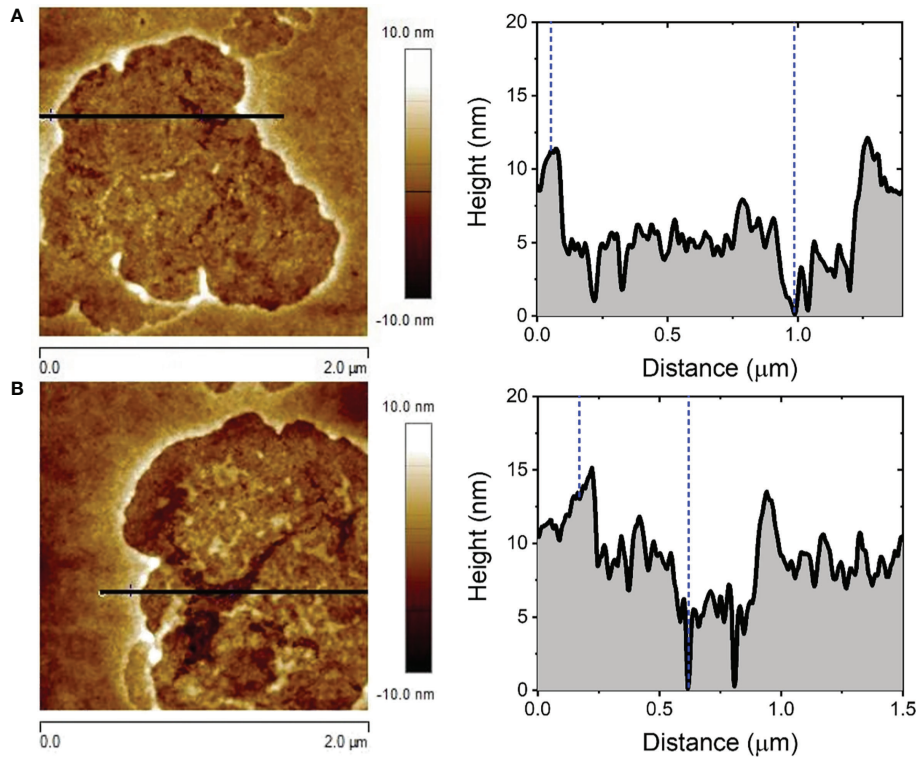


FIGURE 4
2.0 x 2.0 μm² AFM images of the surface of RBC after being exposed to F1 for t = 1 min (A) and t = 30 min (B).

mediate various types of toxicity and bioactivity, such as cardiovascular and respiratory arrest in rats (Hu et al., 2011), lysis of rat, human and sheep erythrocytes (Kohno et al., 2009; Ravindran et al., 2010; Glasser et al., 2014) all caused by a pore-forming mechanism. The mechanism of action of these proteins is penetration through the target cell membrane resulting in diffusion of small molecules and solutes leading to osmotic

imbalance and cell lysis. It requires several steps: *i*) initial binding to the target membrane; *ii*) orientation and consequent oligomerization at the binding site; and *iii*) insertion in the segment to the lipid's membrane and generation of the pore (Parker and Feil, 2005; Saikia et al., 2012). In order to determine the membrane target for PFPs in *M. allicornis* a specific affinity study was carried out. In this

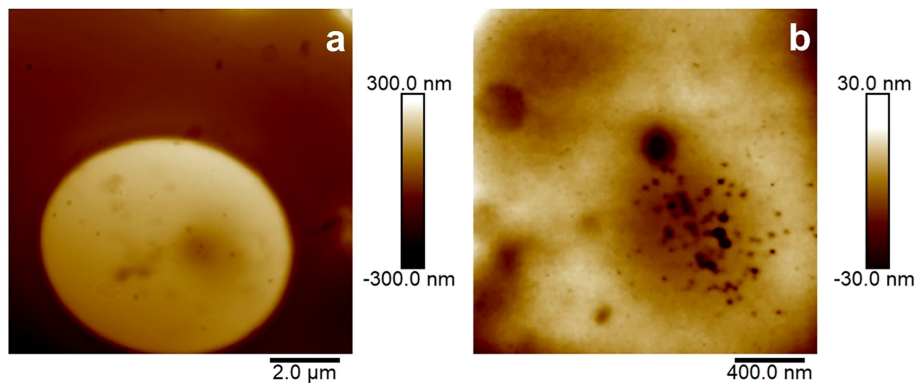


FIGURE 5
10 x 10 μm² (A) and 2.0 x 2.0 μm² (B) AFM images of the surface of RBC after being exposed to alciaporin for t = 1 min.

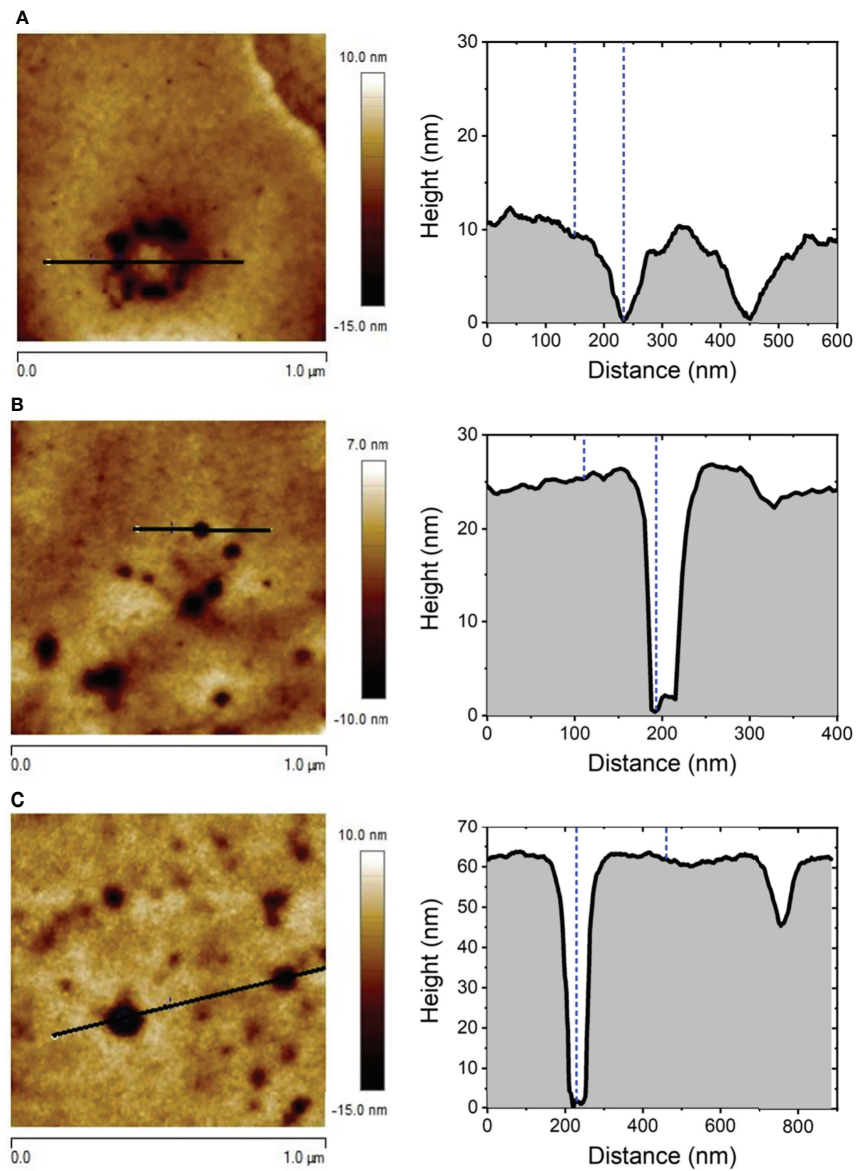


FIGURE 6 Representative cross-section profile of $1.0 \times 1.0 \mu\text{m}^2$ AFM images of the surface of RBC after being exposed to alciporin for $t = 1$ min (A), 5 min (B), and 30 min (C).

TABLE 1 Average RMS roughness, pore diameter and depth obtained from AFM cross section profile of pinholes occurred in RBC membranes after exposure to alciporin for different times.

Sample	Roughness (RMS)/nm	Diameter/nm	Depth/nm
$t = 1$ min	1.74 ± 0.55	37.1 ± 8.3	11.2 ± 3.9
$t = 5$ min	2.52 ± 0.53	51.2 ± 24.6	17.0 ± 8.7
$t = 10$ min	3.32 ± 0.61	68.9 ± 31.9	25.2 ± 13.2
$t = 30$ min	3.78 ± 0.70	78.6 ± 33.6	24.6 ± 13.8

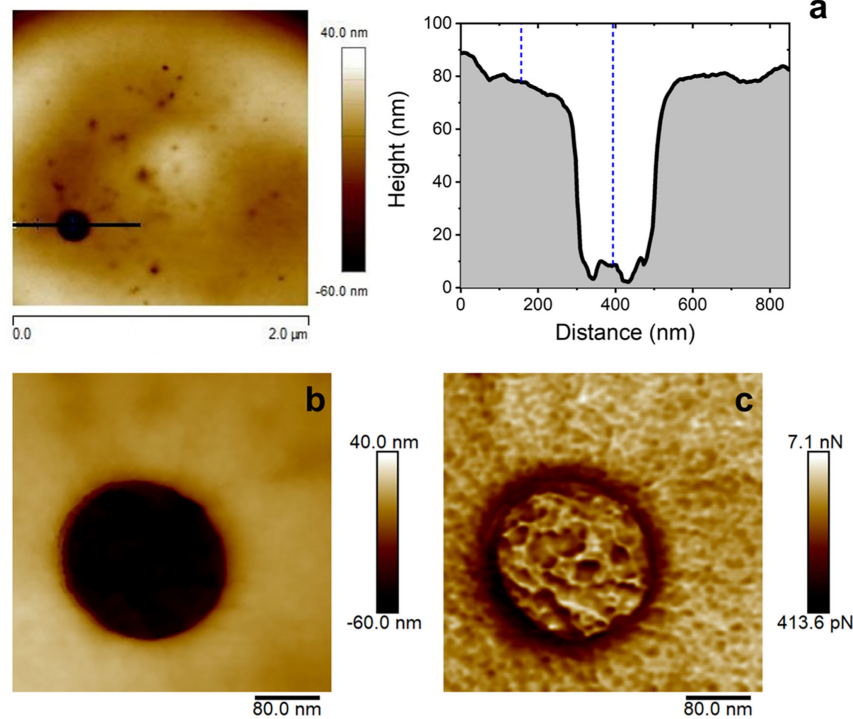


FIGURE 7
Effects observed at the lipid bilayer after 10 min of incubation of rat erythrocyte in the presence of alciporin. AFM image ($2.0 \times 2.0 \mu\text{m}^2$) and cross section of a big pore. Cross sectional profile showing the diameter, depth, and the pore inner ring (A), $400 \times 400 \text{ nm}^2$ AFM detailed images of the pore resembling the morphological features of the cell spectrin cytoskeleton underneath: topographic (B) and adhesion (C) images.

experiment, the percentage of hemolysis of rat erythrocytes at different concentrations of alciporin was analyzed starting from a maximum concentration of 100 $\mu\text{g/mL}$ incubated with commercial sphingomyelin (Sigma) at a 1:1.6 ratio for 60 minutes at 4 °C. Incubation of *M. allicornis* PFP, alciporin, with sphingomyelin reduces hemolytic effects below 10%

(Figure 8). This fact was also corroborated by AFM analysis. Thus, a sample of alciporin was reconstituted in saline solution that containing sphingomyelin. The AFM analysis of hemolytic effects after incubation times of 1, 5, 10 and 30 min showed residual pore formation in the time lapse considered as can be seen in Figures 9; S12, S13.

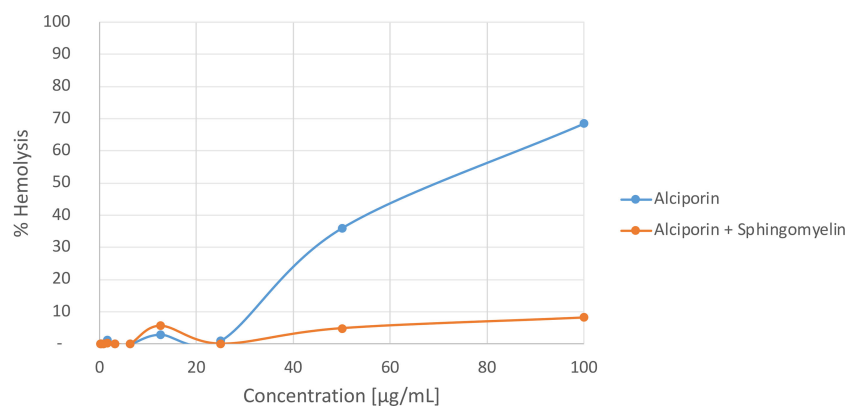


FIGURE 8
Hemolytic activities of alciporin and alciporin + sphingomyelin.

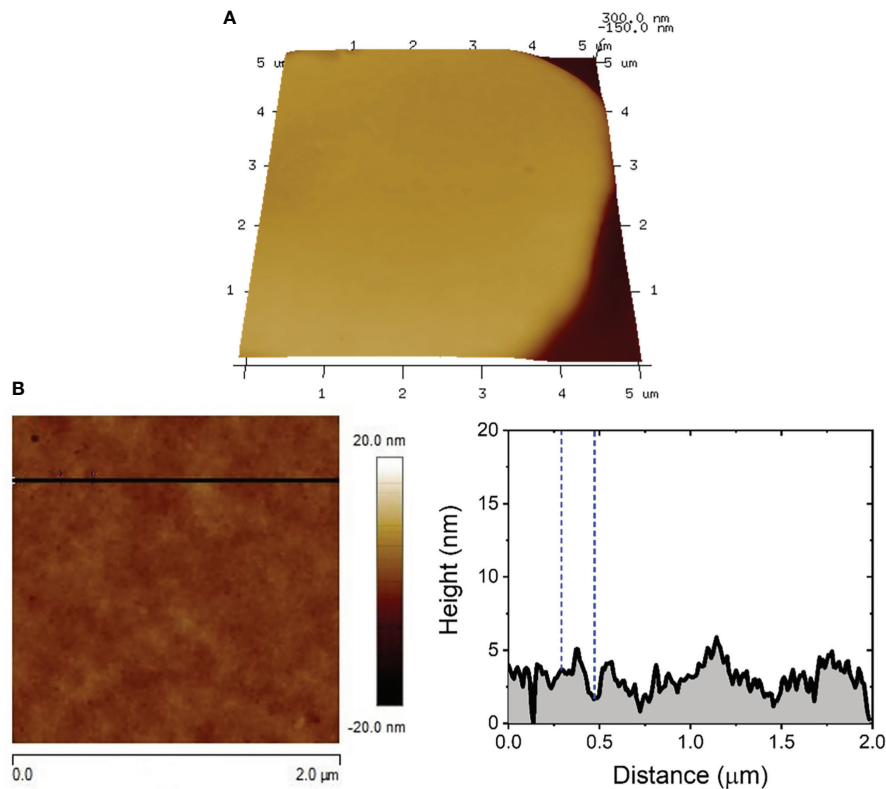


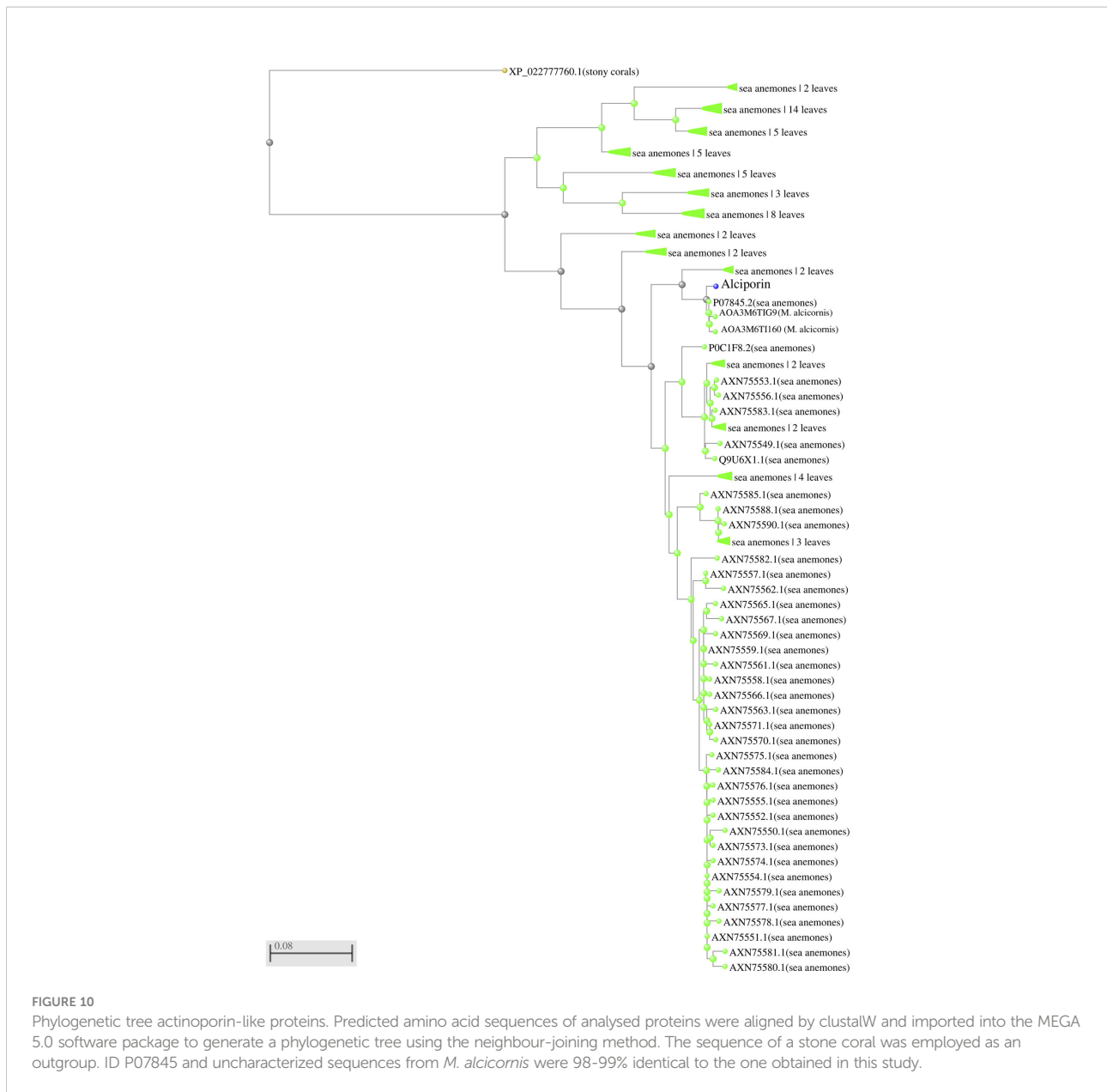
FIGURE 9
5.0 x 5.0 μm² 3D AFM image showing the characteristic topographic features expected for RBCs exposed to alciporin in the presence of sphingomyelin for t = 5 min (A). Cross sectional profile showing the surface roughness of the RBC membrane (B).

Subtle damages observed in the membrane of RBC exposed to alciporin samples in the presence of sphingomyelin, see [Figure S13](#), exhibited morphologies compatible with the activity of residual traces PLA2-type proteins still present in some samples of alciporin. Indeed, the RMS values registered for both unaltered and damaged regions were 0.92 ± 0.28 nm (see [Figures S14, S15](#)) and 1.45 ± 0.36 nm, respectively, with the latter being comparable with those already shown for F1. Occasionally, some isolated pores could be detected only for longer immersion times, [Figure S14](#), whose dimensions (diameter and depth) and surface coverage are significantly lower than those reported for RBC exposed to alciporin in the absence of sphingomyelin. All these results put together confirm that the target of alciporin proteins in the RBC membrane is sphingomyelin.

The sequence of alciporin (F2) was analysed and the identified protein is deposited in the NCBI database under accession number ON158507. The obtained sequences showed 98–99% homology to uncharacterized proteins of *M. alcicornis* available at SwissProt database as well as high levels of homology to actinoporins isolated from other marine species as shown in [Figure 10](#). Hence the obtained sequence of the protein was characterized as an actinoporin of *M. alcicornis*.

Actinoporins are effective, extremely potent PFPs produced by cnidarians. These basic 20 kDa proteins form pores in membranes that contain sphingomyelin ([Hinds et al., 2002](#); [Ramírez-Carretero et al., 2020](#)). The multi-step process of pore formation involves recognition of membrane sphingomyelin, binding to the membrane and the transfer of the N-terminal region to the lipid-water interface to induce pore formation after oligomerization of monomers ([Kristan et al., 2009](#)). Despite most actinoporins produced by sea anemones are a well-studied group of α -PFPs of around 20 kDa comprising an average of 200 aminoacid residues ([Alvarez et al., 2009](#); [Rivera-de-Torre et al., 2018](#); [Ramírez-Carretero et al., 2020](#)), alciporin fit an actinoporin with high homology with the sticholysins family isolated from sea anemones ([Lanio et al., 2001](#)) ([Figure S16](#)). Similar to other described actinoporins, it shows a conserved region of bulky and aromatic aminoacids such as tryptophan or tyrosine usually found at positions 112 and 113, associated with the lipid membrane interaction. Nonetheless, it lacks the highly conserved P-[WYF]-D pattern as well as bulky or aromatic aminoacids ([Kristan et al., 2009](#); [Alvarez et al., 2009](#)).

Based on the AFM analysis, alciporin interacts after 1 min with RBCs lipid membranes that contain sphingomyelin to bind



the bilayer and initiate pore formation. In a second stage, a protein-protein interaction triggers the oligomerization process that leads the formation of toroidal arc pores that range from 25 to 200 nm (Figure S9), as represented in Figure 11.

4 Conclusions

The nematocysts of *M. alicornis* penetrate the human skin and produce lesions similar to burns. The study of nematocysts produced by cnidarian cnidocytes as the main defense mechanism against prey and predators is crucial to understand the stinging effect they have upon contact with the skin. Results

derived from this research work confirmed that the *M. alicornis* aqueous extract contains thermolabile proteins that cause hemolytic effects upon contact, Figure 12. The use of molecular exclusion chromatography and *in vitro* hemolytic assays have allowed us to isolate, detect and monitor two different hemolytic behaviors attributed to the biosynthesis of proteins of the phospholipase A2 (PLA2) and pore forming proteins (PFPs) type, alciporin, as a main defense mechanism. PLA2 catalyzes hydrolysis at the sn-2 position of phospholipids of the phosphatidylcholine type. These enzymes can display different affinities for membranes depending on the phospholipid composition, but mainly for phosphatidylcholine residues in the outer leaflet of the cell membrane. The hydrolysis

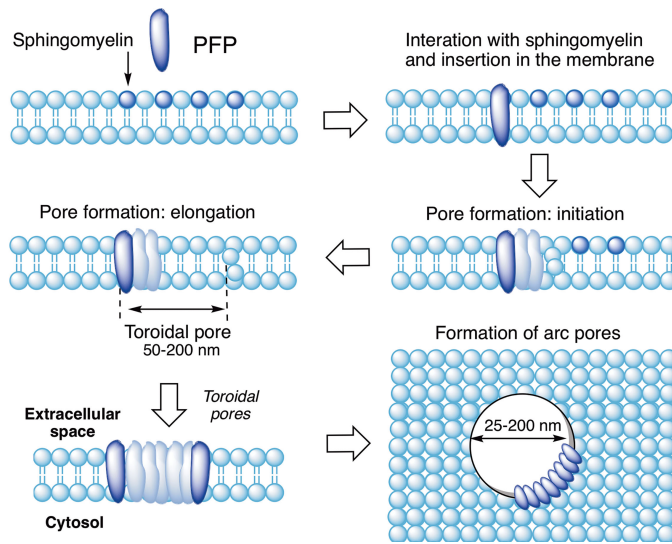


FIGURE 11
Plausible alciporin pore formation mechanism.

reaction triggers a structural damage in the outer leaflet of the lipidic bilayer of RBCs by generating pores that lead the cellular content to flow out of the damaged cells and depletion. Pore-forming proteins (PFPs) target the sphingomyelin of cell membranes, triggering structural damage to the outer/inner

layers of the RBC membrane, generating pores in the lipid bilayer, and potentially leading to cell death and osmotic imbalance. This target has been corroborated by the sphingomyelin inhibition experiment, where it has been possible to confirm through *in vitro* hemolytic assays and by

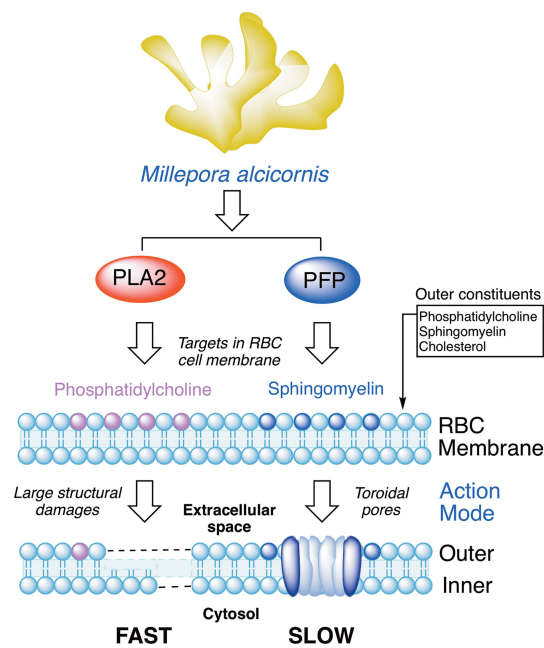


FIGURE 12
Protein-based defense mechanisms observed in *Millepora alcicornis*.

Atomic Force Microscopy (AFM) that the biological target of the PFTs is sphingomyelin, [Figure 9](#). The use of AFM is revealed as a powerful tool to understand biological processes and has allowed us to visualize in detail the mechanisms involved in the damages caused by phospholipase A2 (PLA2) and pore forming proteins (PFTs) of *M. alcinornis* at the nanoscale level. The enormous potential of cnidarian venoms as biological tools for understanding the activity of different receptors and channels in health and disease conditions, as well as their use as sources of novel pharmaceutical lead compounds, such as for the adjunctive therapy for invasive bacterial infection ([Escajadillo and Nizet, 2018](#)), appears to offer endless possibilities for future scientific research ([Benton and Bayly-Jones, 2021](#)). It is important to study the hemolytic properties of cnidarian venoms, which could lead to better care for the victims. In this context we also believe that alcioporin could be a potential candidate to develop biological assays, as the application as antiparasitic agents in which our group is currently working.

Data availability statement

The datasets presented in this study can be found in online repositories. The names of the repository/repositories and accession number (ON158507) can be found below: <https://www.ncbi.nlm.nih.gov/>.

Ethics statement

All animal procedures were performed in accordance guidelines and regulations approved by the Ethical Commission of University of La Laguna (ULL). This study was completed in strict accordance with the authorization and protocol reference number ULL-CEIBA2020-0397.

Author contributions

AD-M, AH-C and JF designed the experiments. AH collected and classified coral specimens. NN conducted coral treatment, protein quantification and hemolytic activity. AG-O and AH-C developed preparation of RBCs samples and AFM analysis. JL-M and RM performed the protein analysis. All authors contributed to the article and approved the submitted version.

Funding

This work was funded by projects PID2019–109476RB-C21 (BIOALGRI) (Spanish Ministry of Science), Madrid, Spain;

Fundación CajaCanarias–Fundación Bancaria “La Caixa” (2019SP52) and Gobierno de Canarias (ProID 2020010123); PI18/01380 from Instituto de Salud Carlos III, Spain and RICET (RD16/0027/0001 project) from Programa Redes Temáticas de Investigación Cooperativa, FIS (Ministerio Español de Salud, Madrid, Spain) and FEDER. (CIBER) de Enfermedades Infecciosas (CIBERINFEC; CB21/13/00100), Instituto de Salud Carlos III, 28006 Madrid, Spain, Ministerio de Sanidad, Consumo y Bienestar, Spain and Cabildo de Tenerife 21/0587 cofunded by MEDI and FDCAN, and EQC2019-005647-P from the Spanish Ministry of Science. NN thanks the Agustín de Betancourt Programme (Cabildo de Tenerife, TFinnova Programme supported by MEDI and FDCAN funds). AG-O thanks NANOTec, INTec, and ULL for laboratory facilities. The proteomic analysis was performed in the proteomics facility of SCSIE University of Valencia that belongs to Proteored, PRB3 and is supported by grant PT17/0019, of the PE I+D+i 2013–2016, funded by ISCIII and ERDF.

Acknowledgments

Authors acknowledge Estabulario (Dr. M.R. Arnau) and AFM Service of General Research Support Services of University of La Laguna (SEGAI-ULL), and the biological activity service of IPNA-CSIC for the analysis of hemolytic activity.

Conflict of interest

The authors declare that the research was conducted in the absence of any commercial or financial relationships that could be construed as a potential conflict of interest.

Publisher's note

All claims expressed in this article are solely those of the authors and do not necessarily represent those of their affiliated organizations, or those of the publisher, the editors and the reviewers. Any product that may be evaluated in this article, or claim that may be made by its manufacturer, is not guaranteed or endorsed by the publisher.

Supplementary material

The Supplementary Material for this article can be found online at: <https://www.frontiersin.org/articles/10.3389/fmars.2022.914084/full#supplementary-material>

References

- Alvarez, C., Mancheño, J. M., Martínez, D., Tejuca, M., Pazos, F., and Lanio, M. E. (2009). Sticholysins, two pore-forming toxins produced by the Caribbean Sea anemone *Stichodactyla helianthus*: their interaction with membranes. *Toxicon* 54 (8), 1135–1147. doi: 10.1016/j.toxicon.2009.02.022
- Bakrač, B., Gutierrez-Aguirre, I., Podlesek, Z., Sonnen, A. F. P., Gilbert, R. J., Maček, P., et al. (2008). Molecular determinants of sphingomyelin specificity of a eukaryotic pore-forming toxin. *J. Biol. Chem.* 283 (27), 18665–18677. doi: 10.1074/jbc.M708747200
- Bax, N., Williamson, A., Agüero, M., Gonzalez, E., and Geeves, W. (2003). Marine invasive alien species: a threat to global biodiversity. *Mar. Pol.* 27, 313–323. doi: 10.1016/S0308-597X(03)00041-1
- Benton, J. T., and Bayly-Jones, C. (2021). Challenges and approaches to studying pore-forming proteins. *Biochem. Soc. Trans.* 49 (6), 2749–2765. doi: 10.1042/BST20210706
- Clemente, S., Rodríguez, A., Brito, A., Ramos, A., Monterroso, O., and Hernández, J. C. (2011). On the occurrence of the hydrocoral *Millepora* (Hydrozoa: milleporidae) in the subtropical eastern Atlantic (Canary islands): is the colonization related to climatic events? *Coral Reefs* 30, 237–240. doi: 10.1007/s00338-010-0681-7
- Díaz-Marrero, A. R., Rodríguez González, M. C., Hernández Creus, A., Rodríguez Hernández, A., and Fernández, J. J. (2019). Damages at the nanoscale on red blood cells promoted by fire corals. *Scientific Reports* 9 (1), 14258. doi: 10.1038/s41598-019-50744-6
- Escajadillo, T., and Nizet, V. (2018). Pharmacological targeting of pore-forming toxins as adjunctive therapy for invasive bacterial infection. *Toxins* 10 (12), 542. doi: 10.3390/toxins10120542
- Espinoza, C., González, M., Mendoza, G., Creus, A. H., Trigos, Á., and Fernández, J. J. (2018). Exploring photosensitization as an efficient antifungal method. *Sci. Rep.* 8 (1), 14489. doi: 10.1038/s41598-018-32823-2
- Fleds, P. A., Graham, J. B., Rosenblatt, R. H., and Somero, G. N. (1993). Effects of expected global climate change on marine faunas. *Trends Ecol. Evol.* 8, 361–367. doi: 10.1016/0169-5347(93)90220-1
- García-Ortega, L., Alegre-Cebollada, J., García-Linares, S., Bruix, M., Martínez-del-Pozo, L., and Gavilanes, J. G. (2011). The behavior of sea anemone actinoporins at the water-membrane interface. *Biochim. Biophys. Acta (BBA) - Biomembr.* 1808 (9), 2275–2288. doi: 10.1016/j.bbmem.2011.05.012
- García-Arredondo, A., Murillo-Esquivel, L. J., Rojas, A., and Sanchez-Rodríguez, J. (2014). Characteristics of hemolytic activity induced by the aqueous extract of the Mexican fire coral *Millepora complanata*. *J. Venom. Anim. Toxins incl. Trop. Dis.* 20, 49. doi: 10.1186/1678-9199-20-49
- Glasser, E., Rachamim, T., Aharonovich, D., and Sher, D. (2014). Hydra actinoporin-like toxin-1, an unusual hemolysin from the nematocyst venom of *Hydra magnipapillata* which belongs to an extended gene family. *Toxicon* 91, 103–113. doi: 10.1016/j.toxicon.2014.04.004
- Harley, C. D. G., Hughes, R. A., Hultgren, K. M., Miner, B. G., Sorte, C. J. B., Thornber, C. S., et al. (2006). The impact of climate change in coastal marine systems. *Ecol. Lett.* 9, 228–241. doi: 10.1111/j.1461-0248.2005.00871.x
- Hernández-Elizarraga, V. H., Ocharán-Mercado, A., Olguín-López, N., Hernández-Matehuala, R., Caballero-Pérez, J., Ibarra-Alvarado, C., et al. (2022). New insights into the toxin diversity and antimicrobial activity of the "Fire coral" *Millepora complanata*. *Toxins* 14 (3), 206. doi: 10.3390/toxins14030206
- Hinds, M. G., Zhang, W., Anderlüh, G., Hansen, P. E., and Norton, R. S. (2002). Solution structure of the eukaryotic pore-forming cytolytic equinatoxin II: implications for pore formation. *J. Mol. Biol.* 315 (5), 1219–1229. doi: 10.1006/jmbi.2001.5321
- Hoeksema, B. W., Nunes, F. L. D., Lindner, A., and De Souza, J. N. (2017). *Millepora alicornis* (Hydrozoa: Capitata) at ascension island: confirmed identity base on morphological and molecular analyses. *J. Mar. Biol. Assoc. UK.* 97, 709–712. doi: 10.1017/S0025315414001283
- Hu, B., Guo, W., Wang, L. H., Wang, J. G., Liu, X. Y., and Jiao, B. H. (2011). Purification and characterization of gigantoxin-4, a new actinoporin from the sea anemone *Stichodactyla gigantea*. *Int. J. Biol. Sci.* 7 (6), 729–739. doi: 10.7150/ijbs.7.729
- Iguchi, A., Iwanaga, S., and Nagai, H. (2008). Isolation and characterization of a novel protein toxin from fire coral. *Biochem. Biophys. Res. Commun.* 365 (1), 107–112. doi: 10.1016/j.bbrc.2007.10.153
- Jouiaei, M., Yanagihara, A., Madio, B., Nevalainen, T., Alewood, P., and Fry, B. (2015). Ancient venom systems: A review on cnidaria toxins. *Toxins* 7 (6), 2251–2271. doi: 10.3390/toxins7062251
- Kohno, Y., Satoh, H., Iguchi, A., and Nagai, H. (2009). Characterization of a new hemolytic protein toxin from the sea anemone *Anthopleura asiatica*. *Fish. Sci.* 75 (4), 1049–1054. doi: 10.1007/s12562-009-0112-2
- Kristan, K. C., Viero, G., Dalla Serra, M., Macek, P., and Anderlüh, G. (2009). Molecular mechanism of pore formation by actinoporins. *Toxicon* 54 (8), 1125–1134. doi: 10.1016/j.toxicon.2009.02.026
- Laborel, J. (1974). West African Reef corals: An hypothesis on their origin. *Proc. 2nd Int. Coral Reef Symp.* 1, 425–443.
- Lanio, M. E., Morera, V., Alvarez, C., Tejuca, M., Gómez, T., Pazos, F., et al. (2001). Purification and characterization of two hemolysins from *Stichodactyla helianthus*. *Toxicon* 39 (2-3), 187–194. doi: 10.1016/S0041-0101(00)00106-9
- Lewis, J. B. (2006). Biology and ecology of the hydrocoral *Millepora* on coral reefs. *Adv. Mar. Biol.* 50, 1–55. doi: 10.1016/S0065-2881(05)50001-4
- Linnaeus, C. (1758). *Systema Naturae per regna tria naturae, secundum classes, ordines, genera, species, cum characteribus, differentiis, synonymis, locis. Editio decima, reformata* [10th revised edition], vol. 1, 824 pp. Laurentius Salvius: Holmiae, Available online at: <https://biodiversitylibrary.org/page/726886>.
- López, C., Clemente, S., Almeida, C., Brito, A., and Hernández, M. (2015). A genetic approach to the origin of millepora sp. in the eastern Atlantic. *Coral Reefs* 34, 631–638. doi: 10.1007/s00338-015-1306-y
- Lourenço, W. R. (2020). The coevolution between telson morphology and venom glands in scorpions (Arachnida). *J. venom. Anim. toxins including Trop. Dis.* 26, e20200128. doi: 10.1590/1678-9199-JVATITD-2020-0128
- Mariottini, G., and Pane, L. (2013). Cytotoxic and cytolytic cnidarian venoms. a review on health implications and possible therapeutic applications. *Toxins* 6 (1), 108–151. doi: 10.3390/toxins6010108
- Olguín-López, N., Heirnandez-Elizarraga, V. H., Hernández-Matehuala, R., Cruz-Hernández, A., Guevara-González, R., Caballero-Pérez, J., et al. (2019). Impact of El Niño-southern oscillation 2015–2016 on the soluble proteomic profile and cytolytic activity of *Millepora alicornis* ("fire coral") from the Mexican Caribbean. *PeerJ* 7, e6593. doi: 10.7717/peerj.6593
- Parker, M. W., and Feil, S. C. (2005). Pore-forming protein toxins: from structure to function. *Prog. Biophys. Mol. Biol.* 88 (1), 91–142. doi: 10.1016/j.pbiomolbio.2004.01.009
- Ramírez-Carreto, S., Miranda-Zaragoza, B., and Rodríguez-Almazán, C. (2020). Actinoporins: From the structure and function to the generation of biotechnological and therapeutic tools. *Biomolecules* 10 (4), 539. doi: 10.3390/biom10040539
- Ravindran, V. S., Kannan, L., and Venkateshvaran, K. (2010). Biological activity of sea anemone proteins: II. cytotoxicity and cell line toxicity. *Indian J. Exp. Biol.* 48, 1233–1236.
- Reyes-Batlle, M., Todd, C. D., Martín-Navarro, C. M., López-Arencibia, A., Cabello-Vilchez, A. M., González, A. C., et al. (2014). Isolation and characterization of *Acanthamoeba* strains from soil samples in gran canaria, canary islands, Spain. *Parasitol. Res.* 113, 1383–1388. doi: 10.1007/s00436-014-3778-z
- Rivera-de-Torre, E., Martínez-Del-Pozo, Á., and Garb, J. E. (2018). *Stichodactyla helianthus* de novo transcriptome assembly: Discovery of a new actinoporin isoform. *Toxicon* 150, 105–114. doi: 10.1016/j.toxicon.2018.05.014
- Rodríguez, A. (2019a). *Experimental studies on the effects of climate change on structural species of marine ecosystems of canary islands* (Congreso Cambio Global de la Macaronesia, Las Palmas de Gran Canaria (oral presentation).
- Rodríguez, A. (2019b). *Ocean warming contributes to arrival and expansion of tropical species* (Congreso Cambio Global de la Macaronesia, Las Palmas de Gran Canaria (oral presentation).
- Rodríguez, L., López, C., Casado-Ameuza, P., Ruiz-Ramos, V., Martínez, B., Banaszak, A., et al. (2019). Genetic relationships of the hydrocoral *Millepora alicornis* and its symbionts within and between locations across the Atlantic. *Coral Reefs* 38, 255–268. doi: 10.1007/s00338-019-01772
- Saikia, D., Bordoloi, N. K., Chattopadhyay, P., Choklingam, S., Ghosh, S. S., and Mukherjee, A. K. (2012). Differential mode of attack on membrane phospholipids by an acidic phospholipase A2 (RVVA-PLA2-I) from *Daboia russelli* venom. *Biochimica et biophysica acta - Biomembranes* 1818 (12), 3149–3157. doi: 10.1016/j.bbmem.2012.08.005
- Shilov, I. V., Seymour, S. L., Patel, A. A., Loboda, A., Tang, W. H., Keating, S. P., et al. (2007). The paragon algorithm, a next generation search engine that uses sequence temperature values and feature probabilities to identify peptides from tandem mass spectra. *Molecular & cellular proteomics. MCP* 6 (9), 1638–1655. doi: 10.1074/mcp.T600050-MCP200
- Tamura, K., Peterson, D., Peterson, N., Stecher, G., Nei, M., and Kumar, S. (2011). MEGA5: molecular evolutionary genetics analysis using maximum

likelihood, evolutionary distance, and maximum parsimony methods. *Mol. Biol. Evol.* 28, 2731–2739. doi: 10.1093/molbev/msr121

Thomsen, M. S., Wernberg, T., and Schiel, D. (2015). “Invasions by non-indigenous species,” in *Marine ecosystems: Human impacts on biodiversity,*

functioning and services. Eds. T. P. Crowe and C. L. J. Frid (Cambridge, UK: Cambridge Univ. Press), 274–331. doi: 10.1017/CBO9781139794763.010

Wirtz, P., and Zilberberg, C. (2019). Fire! the spread of the Caribbean fire coral *Millepora alcicornis* in the Eastern Atlantic. *bioRxiv*. doi: 10.1101/519041